

## ORIGINAL RESEARCH

# Multi-level interval rolling warning method for distributed photovoltaic fluctuation events

Yumin Zhang<sup>1</sup>  | Yunrui Qi<sup>1</sup> | Pingfeng Ye<sup>2</sup>  | Zhengmao Li<sup>3</sup> | Jiajia Yang<sup>4</sup>  | Xingquan Ji<sup>1</sup>

<sup>1</sup>College of Electrical Engineering and Automation, Shandong University of Science and Technology, Qingdao, China

<sup>2</sup>College of Energy Storage Technology, Shandong University of Science and Technology, Qingdao, China

<sup>3</sup>School of Electrical Engineering, Aalto University, Espoo, Finland

<sup>4</sup>College of Science and Engineering, James Cook University, Townsville, Queensland, Australia

## Correspondence

Pingfeng Ye, College of Energy Storage Technology, Shandong University of Science and Technology, Qingdao, China.

Email: ypf@sust.edu.cn

## Funding information

Chinese Postdoctoral Science Foundation, Grant/Award Number: 2023M734092; National Natural Science Foundation of China, Grant/Award Numbers: 52107111, 62403288; Shandong Provincial Natural Science Foundation of China, Grant/Award Numbers: ZR2022ME219, ZR2021QE117, ZR2023QE181, ZR2024ME029

## Abstract

The power fluctuation of distributed photovoltaic (PV) systems significantly impacts the balance of the power system, leading to risks like PV curtailment and load shedding. This paper proposes a multi-level rolling warning method for distributed PV power fluctuation (DPPF) based on interval analysis, aiming to establish a framework for proactively mitigating the potential adverse effects of fluctuations in distributed PV systems. Firstly, the power control mechanism to deal with DPPF is clarified, and warning levels are defined to determine the range of fluctuations that can be controlled by different power control measures. Secondly, based on the probability density of DPPF, the probabilities of each warning level are obtained by integrating the probability densities within each warning range. Finally, the differences in the forecasting accuracy of PV power fluctuations at different time scales are analysed, and the rolling warning of DPPF is achieved by periodically updating PV power output to adjust the warning results. Simulation results demonstrate that the proposed method identifies the thresholds for each warning range and provides warnings for different system operating conditions and PV power fluctuation events, confirming its effectiveness and applicability.

## KEYWORDS

distributed photovoltaic power fluctuation, interval analysis, probability density, rolling warning

## 1 | INTRODUCTION

To accelerate the achievement of the “30–60” goal and promote the low-carbon transformation of energy, China has been increasing its investment in the development of new energy, and the installed capacity of photovoltaic (PV) power has rapidly expanded [1–3]. However, distributed PV generation exhibits strong randomness and volatility [4, 5], leading to increased challenges in handling midday valley and evening peak power supply challenges [6, 7]. This can result in imbalances between power supply and demand as well as insufficient accommodation of distributed PV power [8–10]. Therefore, how to provide advanced warnings for distributed PV power fluctua-

tion (DPPF) events to reduce the risks of PV curtailment and load shedding is an area that needs to be investigated.

Existing power system warning methods can be categorised into statistical learning methods [11, 12] and physical analysis methods [13, 14]. In [11], an early warning method based on a decision tree and semi-supervised deep learning was proposed, which considered dynamic security constraints and wind power uncertainty and could quickly form insecure operating condition sets corresponding to different insecure levels. In [12], a probabilistic risk assessment and early warning model based on Bayesian deep learning was proposed that considered meteorological conditions, aiming to provide warnings for potential extreme weather events and reduce the impact of such events. A

This is an open access article under the terms of the [Creative Commons Attribution-NonCommercial License](https://creativecommons.org/licenses/by-nc/4.0/), which permits use, distribution and reproduction in any medium, provided the original work is properly cited and is not used for commercial purposes.

© 2024 The Author(s). *Energy Conversion and Economics* published by John Wiley & Sons Ltd on behalf of The Institution of Engineering and Technology and the State Grid Economic & Technological Research Institute Co., Ltd.

measurement-based approach was presented in [13] to evaluate potential transient instability issues in a cascading power outage scenario, effectively providing an early warning of impending system instability. The security information index was proposed in [14] to evaluate the static security of a system based on the power flow calculation formula, aiming to identify the current state of the power system, enhance its security, and establish hierarchical thresholds to categorise the severity into four levels. However, because DPPFs often involve “black swan” events, there are technical challenges in the comprehensive and systematic collection of effective fault datasets. Therefore, from the perspective of reliability, it is more appropriate to use physical analysis methods to address the issue of early warning for DPPF; statistical learning methods are not practical.

DPPF can affect primary and secondary frequency regulation, energy storage system charging and discharging, and spinning and non-spinning reserves [15, 16], thereby leading to risks, such as PV curtailment, load shedding, and frequency excursions, which are closely related to power imbalance. Therefore, the aforementioned risk warnings are valuable from the perspective of power balance. For instance, a power balance warning approach for regional grids was presented in [17], where the probability of simultaneity rate compliance was determined using historical data, and a transmission power index was introduced to assess grid stability. Under large-scale PV integration into regional grids, variations in meteorological conditions affect PV output within the affected areas. These clustered power fluctuations are transmitted from the distribution to the transmission networks, significantly increasing the grid frequency regulation requirements [18]. Additionally, compared with centralised PV generation, predicting fluctuations in distributed PV systems is more complex and challenging. Therefore, the effect of DPPF on the power system balance cannot be ignored.

In addition, DPPF is primarily caused by meteorological factors, such as solar irradiance and temperature, which are stochastic and uncertain [18–22]. The typically used methods to address uncertainties in power systems include the scenario [23], robust optimisation [24], and interval analysis methods [25, 26]. The scenario method simulates uncertainties by generating several scenarios through sampling, which requires knowledge of the probability distributions of the variables. However, this is computationally intensive and often impractical for early warning systems that require a timely response. The robust optimisation method makes optimal decisions based on the worst-case scenario of uncertain parameters, resulting in lower computational demands but overly conservative outcomes, making it less suitable for warning systems because of its one-sided results. In contrast, the interval analysis method describes variables in the form of interval numbers, which have lower computational requirements and more comprehensive results than robust optimisation methods. A Bayesian optimisation-based time-series forecasting algorithm was proposed in [25], which used interval analysis to obtain probability prediction intervals for PV power generation under 15% to 95% confidence levels. In [26], a hybrid interval forecasting

model was developed based on fuzzy information granulation, an improved long- and short-term memory network, and an autoregressive moving average to predict the interval of PV output power, which can accurately cover the actual PV power and deliver more valuable decision information for power system dispatching. This method is suitable for solving optimal dispatching problems using the variable-range information alone. Currently, providing an accurate probability distribution of the PV output for DPPF events remains challenging [27, 28]. This aligns with the application scenario of interval analysis, in which interval numbers can be used to represent the uncertainty of PV power fluctuations.

Therefore, to address the aforementioned issues, this study focuses on the power balance in the power system and incorporates interval analysis into DPPF warnings. Based on the effectiveness of different power regulation measures on DPPF events, a multi-level interval rolling warning method is proposed, aiming to reduce risks, such as PV curtailment, load shedding, and frequency excursions. The primary contributions of this study are as follows:

- 1) A multi-level warning method for DPPF events is proposed. This method aims to achieve power balance and divides the warning levels based on the effectiveness of different power regulation measures. Five levels of warning were defined based on the severity of the DPPF events.
- 2) Considering the uncertainty of the PV power, interval numbers were used to represent the DPPF. The probability density of the DPPF within each warning interval was determined, and warning probabilities were calculated. A rolling warning approach was proposed that uses the latest PV prediction data to adjust the warning results, thereby improving the accuracy of long-term warnings.

## 2 | ALLOWABLE RANGE OF PV POWER FLUCTUATION AMPLITUDE

The foremost power regulation measures in power systems include primary frequency control, secondary frequency control, energy storage system charging and discharging, spinning reserves, non-spinning reserves, solar power curtailment, and demand response initiatives, such as load shedding. This section evaluates the effectiveness of different power regulation measures derives acceptable thresholds for the amplitude of the fluctuations in the distributed PV output that can be equilibrated via each power control mechanism across different time periods.

### 2.1 | Automation of power control in power systems

Implementing automatic frequency control is crucial for maintaining the power balance of power systems, particularly when the distributed PV power fluctuates frequently.

### 2.1.1 | Primary frequency control

According to the power balance condition, the power changes of the generator and load satisfy:

$$-\sum_{i=1}^{N_G} \frac{1}{\delta_i} \Delta f + \Delta P_t^{\text{PV}} = \Delta P_t^{\text{L}} + K^{\text{L}} \Delta f, \quad (1)$$

where  $N_G$ ,  $\delta_i$ ,  $\Delta f$ ,  $\Delta P_t^{\text{PV}}$ ,  $\Delta P_t^{\text{L}}$ , and  $K^{\text{L}}$  represent the number of conventional units, unit's regulation rate, static frequency deviation, magnitude of PV power fluctuation, the load prediction deviation, and load's frequency regulation effect coefficient, respectively.

The composite frequency regulation effect coefficient of the system is

$$K = \sum_{i=1}^{N_G} \frac{1}{\delta_i} + K^{\text{L}}. \quad (2)$$

We used interval arithmetic to determine the allowable range of PV power fluctuation amplitude so that power balance can be achieved with one frequency regulation action alone, which can be expressed as

$$[\Delta \underline{P}_t^{\text{pv1}}, \Delta \overline{P}_t^{\text{pv1}}] = \Delta P_t^{\text{L}} + K [\Delta f^{\text{min}}, \Delta f^{\text{max}}]; \quad (3)$$

$$\Delta \underline{P}_t^{\text{pv1}} = \Delta \underline{P}_t^{\text{L}} + K \Delta f^{\text{min}}; \quad (4)$$

$$\Delta \overline{P}_t^{\text{pv1}} = \Delta \overline{P}_t^{\text{L}} + K \Delta f^{\text{max}}, \quad (5)$$

where  $\Delta \overline{P}_t^{\text{pv1}}$  and  $\Delta \underline{P}_t^{\text{pv1}}$  represent the upper and lower limits of the allowable range of PV power fluctuation amplitudes at time  $t$ , respectively.  $\Delta \overline{P}_t^{\text{L}}$  and  $\Delta \underline{P}_t^{\text{L}}$  represent the upper and lower bounds of the load power change caused by load-forecasting errors at time  $t$ , respectively.  $\Delta f^{\text{max}}$  and  $\Delta f^{\text{min}}$  represent the upper and lower limits of the allowable system frequency deviation, respectively.

As long as the PV power fluctuation amplitude falls within the interval  $[\Delta \underline{P}_t^{\text{pv1}}, \Delta \overline{P}_t^{\text{pv1}}]$ , power balance can be achieved with just one frequency regulation action.

Considering the load prediction error, when calculating the upper and lower limits of the PV power fluctuation range according to Equations (4) and (5), the upper and lower boundary values of the load power change should be used to ensure that the power balance condition is satisfied within the error range.

### 2.1.2 | Secondary frequency control

When power regulation capability of the primary frequency regulator is insufficient to independently address DPPF events, secondary frequency regulation is required to further adjust the

output of the units to achieve power balance. According to the power-balance condition, we obtain

$$-\sum_{i=1}^{N_G} \frac{1}{\delta_i} \Delta f + \sum_{j=1}^{N_{\text{AGC}}} \Delta P_{j,t} + \Delta P_t^{\text{PV}} = \Delta P_t^{\text{L}} + K^{\text{L}} \Delta f, \quad (6)$$

where  $N_{\text{AGC}}$  represents the total number of automatic generation control (AGC) units, and  $\Delta P_{j,t}$  represents the output adjustment of unit  $j$  at time  $t$ .

By applying interval arithmetic rules, we can obtain the allowable range of PV power fluctuation amplitudes when both the primary and secondary frequency regulations are in effect, ensuring the condition of power balance is met, as

$$[\Delta \underline{P}_t^{\text{pv2}}, \Delta \overline{P}_t^{\text{pv2}}] = \Delta P_t^{\text{L}} - \sum_{j=1}^{N_{\text{AGC}}} [\Delta P_{j,t}^{\text{max}}, \Delta P_{j,t}^{\text{min}}] + K [\Delta f^{\text{min}}, \Delta f^{\text{max}}]; \quad (7)$$

$$\Delta \underline{P}_t^{\text{pv2}} = \Delta \underline{P}_t^{\text{L}} - \sum_{j=1}^{N_{\text{AGC}}} \Delta P_{j,t}^{\text{max}} + K \Delta f^{\text{min}}; \quad (8)$$

$$\Delta \overline{P}_t^{\text{pv2}} = \Delta \overline{P}_t^{\text{L}} - \sum_{j=1}^{N_{\text{AGC}}} \Delta P_{j,t}^{\text{min}} + K \Delta f^{\text{max}}, \quad (9)$$

where  $\Delta \overline{P}_t^{\text{pv2}}$  and  $\Delta \underline{P}_t^{\text{pv2}}$  respectively represent the upper and lower limits of the allowable range of DPPF amplitudes at time  $t$  when secondary frequency regulation is involved. As long as the PV power fluctuation amplitude falls within the interval  $[\Delta \underline{P}_t^{\text{pv2}}, \Delta \overline{P}_t^{\text{pv2}}]$ , the system can achieve power balance through the combined action of the primary and secondary frequency regulations.  $\Delta P_{j,t}^{\text{min}}$  and  $\Delta P_{j,t}^{\text{max}}$  represent the minimum and maximum adjustments of the AGC unit  $j$  at time  $t$ , respectively, which can be expressed as

$$\Delta P_{j,t}^{\text{max}} = \min \left\{ P_j^{\text{max}} - P_{j,0}, \Delta P_{j,(t-\Delta t)}^{\text{real,min}} + R_j \Delta t \right\}; \quad (10)$$

$$\Delta P_{j,t}^{\text{min}} = \max \left\{ P_j^{\text{min}} - P_{j,0}, \Delta P_{j,(t-\Delta t)}^{\text{real,max}} - R_j \Delta t \right\}, \quad (11)$$

where  $P_j^{\text{min}}$  and  $P_j^{\text{max}}$  represent the minimum and maximum allowable outputs of the AGC unit, respectively;  $P_{j,0}$  represents the initial outputs of the AGC unit  $j$  when the warning occurs;  $\Delta P_{j,(t-\Delta t)}^{\text{real,min}}$  and  $\Delta P_{j,(t-\Delta t)}^{\text{real,max}}$  respectively represent the upper and lower limits of the actual adjustment of the AGC unit  $j$  at the previous period, which can be expressed as

$$\Delta P_{j,(t-\Delta t)}^{\text{real,min}} = \max \left\{ \Delta P_{j,(t-\Delta t)}^{\text{min}}, \Delta P_{j,(t-\Delta t)}^{\text{ideal,min}} \right\}, \quad (12)$$

$$\Delta P_{j,(t-\Delta t)}^{\text{real,max}} = \min \left\{ \Delta P_{j,(t-\Delta t)}^{\text{max}}, \Delta P_{j,(t-\Delta t)}^{\text{ideal,max}} \right\}, \quad (13)$$

where  $\Delta P_{j,(t-\Delta t)}^{\text{ideal,max}}$  and  $\Delta P_{j,(t-\Delta t)}^{\text{ideal,min}}$  respectively represent the upper and lower limits of the ideal adjustment of AGC unit  $j$  determined by the deviation of the load forecast at time  $t - \Delta t$

and the actual PV power fluctuations. The overall adjustment range of all AGC units is determined by the deviation of the load forecast and actual fluctuations of the distributed PV, which can be written as

$$\sum_{j=1}^{N_{AGC}} \Delta P_{j,(t-\Delta t)}^{\text{ideal,min}} = \Delta P_{-(t-\Delta t)}^L + K \Delta f^{\text{min}} - \Delta \bar{P}_{(t-\Delta t)}^{\text{pv}}; \quad (14)$$

$$\sum_{j=1}^{N_{AGC}} \Delta P_{j,(t-\Delta t)}^{\text{ideal,max}} = \Delta \bar{P}_{(t-\Delta t)}^L + K \Delta f^{\text{max}} - \Delta P_{-(t-\Delta t)}^{\text{pv}}. \quad (15)$$

From (10)–(15), it is evident that in the entire regulation process, the ideal adjustment of the AGC units that can achieve power balance at time  $t - \Delta t$  should initially be calculated using (14) and (15):

## 2.2 | Charging and discharging processes of energy storage systems

Due to the limited foresight in predicting DPPF, relying solely on primary and secondary frequency regulation methods may lead to challenges in maintaining power balance during significant PV power fluctuation. This in turn affects the frequency stability of the system. In such cases, it is necessary to consider the discharging or charging of energy storage systems to achieve power balance.

Based on the power balance conditions, it can be determined that:

$$-\sum_{i=1}^{N_G} \frac{1}{\delta_i} \Delta f + \Delta P_t^{\text{ESS}} + \sum_{j=1}^{N_{AGC}} \Delta P_{j,t} + \Delta P_t^{\text{pv}} = \Delta P_t^L + K^L \Delta f, \quad (16)$$

where  $\Delta P_t^{\text{ESS}}$  represents the output of the energy storage system at time  $t$ . It is crucial to consider scenarios in which the energy storage system is depleted or fully charged.

Transforming Equation (16) into interval form, we get

$$\begin{aligned} [\Delta P_{-t}^{\text{pv}3}, \Delta \bar{P}_t^{\text{pv}3}] &= \Delta P_t^L - [\Delta P_t^{\text{ESS,max}}, \Delta P_t^{\text{ESS,min}}] \\ &\quad - \sum_{j=1}^{N_{AGC}} [\Delta P_{j,t}^{\text{max}}, \Delta P_{j,t}^{\text{min}}] \\ &\quad + K [\Delta f^{\text{min}}, \Delta f^{\text{max}}]; \end{aligned} \quad (17)$$

$$\Delta P_{-t}^{\text{pv}3} = \Delta \bar{P}_t^L - \Delta P_t^{\text{ESS,max}} - \sum_{j=1}^{N_{AGC}} \Delta P_{j,t}^{\text{max}} + K \Delta f^{\text{min}}; \quad (18)$$

$$\Delta \bar{P}_t^{\text{pv}3} = \Delta P_{-t}^L - \Delta P_t^{\text{ESS,min}} - \sum_{j=1}^{N_{AGC}} \Delta P_{j,t}^{\text{min}} + K \Delta f^{\text{max}}, \quad (19)$$

where  $\Delta \bar{P}_t^{\text{pv}3}$  and  $\Delta P_{-t}^{\text{pv}3}$  represent the upper and lower limits of the permissible interval for the DPPF at time  $t$ , respectively,

when secondary frequency regulation and the energy storage system are involved. As long as the PV power fluctuation amplitude remains within this interval  $[\Delta P_{-t}^{\text{pv}3}, \Delta \bar{P}_t^{\text{pv}3}]$ , the system can achieve power balance through automatic power control and the charging and discharging of energy storage systems.  $\Delta P_t^{\text{ESS,max}}$  and  $\Delta P_t^{\text{ESS,min}}$  denote the maximum and minimum outputs of the energy storage system at time  $t$ , respectively. The calculation process can be expressed as

$$\Delta P_t^{\text{ESS,max}} = \begin{cases} 0, \\ E_{t-\Delta t}^{\text{ESS}} \leq 0 \text{ or } \Delta \bar{P}_{-t}^{\text{pv}2} \leq \Delta \bar{P}_{-t}^{\text{pv}} \\ \min \{ \eta^{\text{dis}} E_{t-\Delta t}^{\text{ESS}}, P^{\text{ESS,max}} \}, \\ E_{t-\Delta t}^{\text{ESS}} > 0 \text{ and } \Delta \bar{P}_{-t}^{\text{pv}2} > \Delta \bar{P}_{-t}^{\text{pv}} \end{cases}; \quad (20)$$

$$\Delta P_t^{\text{ESS,min}} = \begin{cases} 0, \\ E_t^{\text{ESS}} \geq E_{\text{max}}^{\text{ESS}} \text{ or } \Delta \bar{P}_t^{\text{pv}2} \geq \Delta \bar{P}_t^{\text{pv}} \\ \max \{ (E_{t-1}^{\text{ESS}} - E_{\text{max}}^{\text{ESS}}) / \eta^{\text{char}}, P^{\text{ESS,min}} \}, \\ E_t^{\text{ESS}} < E_{\text{max}}^{\text{ESS}} \text{ and } \Delta \bar{P}_t^{\text{pv}2} < \Delta \bar{P}_t^{\text{pv}} \end{cases}; \quad (21)$$

$$E_{t-\Delta t}^{\text{ESS}} = E_0^{\text{ESS}} - \frac{1}{\eta^{\text{dis}}} \sum_{\tau=\Delta t}^{t-\Delta t} \Delta P_{\tau}^{\text{ESS,max}} \Delta t - \eta^{\text{char}} \sum_{\tau=\Delta t}^{t-\Delta t} \Delta P_{\tau}^{\text{ESS,min}} \Delta t, \quad (22)$$

where  $E_t^{\text{ESS}}$  represents the remaining capacity of the energy storage system at time  $t$ .  $E_{\text{max}}^{\text{ESS}}$  denotes the maximum capacity of the energy storage system, and  $\eta^{\text{char}}$  and  $\eta^{\text{dis}}$  represent the charging and discharging efficiency of the energy storage system, respectively.  $\Delta \bar{P}_t^{\text{pv}}$  and  $\Delta P_{-t}^{\text{pv}}$  represent the upper and lower limits, respectively, of the predicted output interval of the distributed PV system.

## 2.3 | Process of active power control in power system

Owing to the limited lead time for forecasting PV power fluctuations, achieving power balance solely through automatic frequency regulation and the charging and discharging of energy storage systems may become challenging during intense PV power fluctuations, potentially affecting the stability of the system frequency. In such cases, reserve capacity must be scheduled to achieve power balance, including spinning and non-spinning reserves.

### 2.3.1 | Spinning reserve

We increase the use of spinning reserves by issuing dispatch instructions to adjust the output of non-AGC units, thereby enhancing the power regulation capability. According to the

power-balance condition, we obtain

$$\begin{aligned} & - \sum_{i=1}^{N_G} \frac{1}{\delta_i} \Delta f + \Delta P_t^{\text{ESS}} + \sum_{j=1}^{N_{\text{AGC}}} \Delta P_{j,t} + \sum_{m=1}^{N_{\text{TMSR}}} \Delta P_{m,t} + \Delta P_t^{\text{PV}} \\ & = \Delta P_t^{\text{L}} + K^{\text{L}} \Delta f, \end{aligned} \quad (23)$$

where  $N_{\text{TMSR}}$  represents the number of units participating in the spinning reserves, and  $\Delta P_{m,t}$  represents the adjustment of the output power of the spinning reserve unit  $m$ .

By applying interval arithmetic rules, we can obtain the allowable range of PV power fluctuation amplitudes when the system achieves power balance through the simultaneous use of automatic frequency control and spinning reserve scheduling, which can be expressed as

$$\begin{aligned} [\Delta P_{-t}^{\text{pv}4}, \Delta P_{-t}^{\text{pv}4}] & = \Delta P_t^{\text{L}} - \sum_{m=1}^{N_{\text{TMSR}}} [\Delta P_{m,t}^{\text{max}}, \Delta P_{m,t}^{\text{min}}] \\ & \quad - [\Delta P_t^{\text{ESS,min}}, \Delta P_t^{\text{ESS,max}}] \\ & \quad - \sum_{j=1}^{N_{\text{AGC}}} [\Delta P_{j,t}^{\text{max}}, \Delta P_{j,t}^{\text{min}}] \\ & \quad + K [\Delta f^{\text{min}}, \Delta f^{\text{max}}]; \end{aligned} \quad (24)$$

$$\begin{aligned} \Delta P_{-t}^{\text{pv}4} & = \Delta P_t^{\text{L}} - \sum_{m=1}^{N_{\text{TMSR}}} \Delta P_{m,t}^{\text{max}} - \Delta P_t^{\text{ESS,max}} - \sum_{j=1}^{N_{\text{AGC}}} \Delta P_{j,t}^{\text{max}} \\ & \quad + K \Delta f^{\text{min}}; \end{aligned} \quad (25)$$

$$\begin{aligned} \Delta P_{-t}^{\text{pv}4} & = \Delta P_t^{\text{L}} - \sum_{m=1}^{N_{\text{TMSR}}} \Delta P_{m,t}^{\text{min}} - \Delta P_t^{\text{ESS,min}} - \sum_{j=1}^{N_{\text{AGC}}} \Delta P_{j,t}^{\text{min}} \\ & \quad + K \Delta f^{\text{max}}; \end{aligned} \quad (26)$$

where  $\Delta P_{-t}^{\text{pv}4}$  and  $\Delta P_{-t}^{\text{pv}4}$  represent the upper and lower limits, respectively, of the allowable range of PV power fluctuation amplitudes at time  $t$  when both secondary frequency regulation and spinning reserves are involved. As long as the PV power fluctuation amplitude falls within the interval  $[\Delta P_{-t}^{\text{pv}4}, \Delta P_{-t}^{\text{pv}4}]$ , the system can achieve power balance through automatic power control and spinning reserves.  $\Delta P_{m,t}^{\text{min}}$  and  $\Delta P_{m,t}^{\text{max}}$ , respectively, represent the minimum and maximum adjustment of spinning reserve units  $m$  at time  $t$ , which can be expressed as

$$\Delta P_{k,t}^{\text{max}} = \min \left\{ P_k^{\text{max}} - P_{k,0}, \Delta P_{k,(t-\Delta t)}^{\text{real,min}} + R_k \Delta t \right\}; \quad (27)$$

$$\Delta P_{k,t}^{\text{min}} = \max \left\{ P_k^{\text{min}} - P_{k,0}, \Delta P_{k,(t-\Delta t)}^{\text{real,max}} - R_k \Delta t \right\}, \quad (28)$$

where  $k$  represents the sum of AGC and spinning reserve units;  $\Delta P_{k,t}^{\text{min}}$  and  $\Delta P_{k,t}^{\text{max}}$  represent the minimum and maximum adjustments of AGC or spinning reserve units, respectively;  $P_k^{\text{min}}$  and  $P_k^{\text{max}}$  represent the minimum and maximum allowable

outputs of unit  $k$ , respectively;  $P_{k,0}$  represents the initial output of unit  $k$  when the warning occurs, and  $\Delta P_{k,(t-\Delta t)}^{\text{real,max}}$  and  $\Delta P_{k,(t-\Delta t)}^{\text{real,min}}$  represent the upper and lower limits, respectively, of the actual adjustment of unit  $k$  at time  $t - \Delta t$ , which are similarly affected by the regulating variable and real-time PV power fluctuations. They can also be calculated similarly to Equations (12) to (15).

### 2.3.2 | Non-spinning reserve and shutdown

When automatic frequency regulation and spinning reserve fail to achieve power balance, the non-spinning units should be started immediately in response to downward PV power fluctuations to mitigate the risk of load shedding. Conversely, some units should be shut down in the case of upward PV power fluctuations to prevent PV curtailment. Based on the power balance condition, we have

$$\begin{aligned} & - \sum_{i=1}^{N_G} \frac{1}{\delta_i} \Delta f + \sum_{j=1}^{N_{\text{AGC}}} \Delta P_{j,t} + \Delta P_t^{\text{ESS}} + \sum_{m=1}^{N_{\text{TMSR}}} \Delta P_{m,t} \\ & \quad + \sum_{n=1}^{N_{\text{TMNSR}}} \Delta P_{n,t} + \Delta P_t^{\text{PV}} = \Delta P_t^{\text{L}} + K^{\text{L}} \Delta f, \end{aligned} \quad (29)$$

where  $N_{\text{TMNSR}}$  represents the total number of non-spinning reserve units and turned-off units, and  $\Delta P_{n,t}$  represents the power adjustment of the non-spinning reserve or shutdown unit  $n$ .

Simplifying and transforming Equation (29) into interval form, we have

$$\begin{aligned} [\Delta P_{-t}^{\text{pv}5}, \Delta P_{-t}^{\text{pv}5}] & = \Delta P_t^{\text{L}} - \sum_{n=1}^{N_{\text{TMNSR}}} [\Delta P_{n,t}^{\text{max}}, \Delta P_{n,t}^{\text{min}}] \\ & \quad - \sum_{m=1}^{N_{\text{TMSR}}} [\Delta P_{m,t}^{\text{max}}, \Delta P_{m,t}^{\text{min}}] \\ & \quad - [\Delta P_t^{\text{ESS,min}}, \Delta P_t^{\text{ESS,max}}] \\ & \quad - \sum_{j=1}^{N_{\text{AGC}}} [\Delta P_{j,t}^{\text{max}}, \Delta P_{j,t}^{\text{min}}] \\ & \quad + K [\Delta f^{\text{min}}, \Delta f^{\text{max}}]; \end{aligned} \quad (30)$$

$$\begin{aligned} \Delta P_{-t}^{\text{pv}5} & = \Delta P_t^{\text{L}} - \sum_{n=1}^{N_{\text{TMNSR}}} \Delta P_{n,t}^{\text{max}} - \sum_{m=1}^{N_{\text{TMSR}}} \Delta P_{m,t}^{\text{max}} \\ & \quad - \Delta P_t^{\text{ESS,max}} - \sum_{j=1}^{N_{\text{AGC}}} \Delta P_{j,t}^{\text{max}} + K \Delta f^{\text{min}}; \end{aligned} \quad (31)$$

$$\begin{aligned} \Delta P_{-t}^{\text{pv}5} & = \Delta P_t^{\text{L}} - \sum_{n=1}^{N_{\text{TMNSR}}} \Delta P_{n,t}^{\text{min}} - \sum_{m=1}^{N_{\text{TMSR}}} \Delta P_{m,t}^{\text{min}} \\ & \quad - \Delta P_t^{\text{ESS,min}} - \sum_{j=1}^{N_{\text{AGC}}} \Delta P_{j,t}^{\text{min}} + K \Delta f^{\text{max}}, \end{aligned} \quad (32)$$

where  $\Delta P_{n,t}^{\max}$  and  $\Delta P_{n,t}^{\min}$  represent the maximum and minimum power adjustments of the non-spinning reserve or shutdown unit  $n$ , respectively. There are primarily affected by the minimum startup/shutdown time of the unit, which can be expressed as

$$\Delta P_{n,t}^{\max} = P_n^{\max} f_{n,t}^{\text{on}}, \quad (33)$$

$$f_{n,t}^{\text{on}} = \begin{cases} 1 & t - t_0 \geq t_n^{\text{on}} \\ 0 & t - t_0 < t_n^{\text{on}} \end{cases}; \quad (34)$$

$$\Delta P_{n,t}^{\min} = -P_n^{\min} f_{n,t}^{\text{off}} \quad (35)$$

$$f_{n,t}^{\text{off}} = \begin{cases} 1 & t - t_0 \geq t_n^{\text{off}} \\ 0 & t - t_0 < t_n^{\text{off}} \end{cases}, \quad (36)$$

where  $P_n^{\max}$  and  $P_n^{\min}$ , respectively, represent the maximum and minimum allowable output power of unit  $n$ .  $f_{n,t}^{\text{on}}$  is a binary variable indicating whether unit  $n$  can complete startup at time  $t$ , depending on the startup time  $t_n^{\text{on}}$  of unit  $n$ , with a value of one indicating the completion of the startup. Similarly,  $f_{n,t}^{\text{off}}$  is a binary variable indicating whether unit  $n$  can complete shutdown at time  $t$ .

## 2.4 | Process of forced power balancing of power systems

When the aforementioned measures fail to satisfy the power balance condition, it becomes necessary to implement load shedding to address the downward PV power fluctuation or curtailment to address the upward PV power fluctuation. The forced power balancing situation can be expressed as

$$\begin{aligned} & -\sum_i^{N_G} \frac{1}{\delta_i} \Delta f_t + \Delta P_t^{\text{ESS}} + \sum_i^{N_G} \Delta P_{i,t} + \Delta P_t^{\text{PV}} - \Delta P_t^{\text{PV,curt}} \\ & = \Delta P_t^{\text{L}} - \Delta P_t^{\text{L,shed}} + K \Delta f_t, \end{aligned} \quad (37)$$

where  $\Delta P_t^{\text{PV,curt}}$  represents the curtailed PV power, and  $\Delta P_t^{\text{L,shed}}$  represents the load power shed.

Assuming that the installed capacity of the PV generation is  $P^{\text{PV,max}}$ , and the PV output power before the fluctuation event is  $P_0^{\text{PV}}$ , it can be inferred that the maximum fluctuation is  $P^{\text{PV,max}} - P_0^{\text{PV}}$  or  $-P_0^{\text{PV}}$ .

## 3 | ROLLING EARLY WARNING PROCESS OF DPPF

### 3.1 | Classification of multi-level early warning for PV power fluctuation events

When the allowable amplitude ranges of the DPPF corresponding to different power control measures are determined, different early warning levels can be established and compared with the predicted values of the DPPF to achieve a hierarchi-

cal early warning. In this study, based on the severity of the impact of DPPF events on the stability of the power system, five warning levels were classified as follows:

- 1) When  $\Delta P_t^{\text{PV}} \in [\Delta P_t^{\text{PV}1}, \Delta P_t^{\text{PV}1}]$  indicates a relatively small amplitude, the primary frequency regulation measure is sufficient to achieve a power balance. Simultaneously, by adjusting the AGC units, the system frequency quickly returns to the rated value. Therefore, this DPPF event has minimal impact on the stability of the power system and does not require an alarm.
- 2) When  $\Delta P_t^{\text{PV}} \in [\Delta P_t^{\text{PV}2}, \Delta P_t^{\text{PV}1}] \cup [\Delta P_t^{\text{PV}1}, \Delta P_t^{\text{PV}2}]$  indicates a moderate amplitude, both primary and secondary frequency regulation measures are required to achieve a power balance. During the regulation process, it is necessary to continuously monitor the operational status of the AGC units. Therefore, DPPF events in this range have a minor impact on the stability of the power system and require only a Level IV warning.
- 3) When  $\Delta P_t^{\text{PV}} \in [\Delta P_t^{\text{PV}3}, \Delta P_t^{\text{PV}2}] \cup [\Delta P_t^{\text{PV}2}, \Delta P_t^{\text{PV}3}]$ , the DPPF is significant. During this period, automatic control measures alone cannot achieve power balance, necessitating the adjustment of power by the energy storage system to maintain balance. The activation of the energy storage system requires manual operation. Considering the cost and backup capacity limitations of energy storage systems [29, 30], DPPF events within this interval were classified as Level IV warnings.
- 4) During  $\Delta P_t^{\text{PV}} \in [\Delta P_t^{\text{PV}4}, \Delta P_t^{\text{PV}3}] \cup [\Delta P_t^{\text{PV}3}, \Delta P_t^{\text{PV}4}]$ , automatic control measures and energy storage methods are insufficient to achieve a power balance. Hence, operators must dispatch spinning reserve units to achieve power balance. Therefore, PV power fluctuation events in this range significantly impact the stability of the power system, warranting Level III warnings.
- 5) When  $\Delta P_t^{\text{PV}} \in [\Delta P_t^{\text{PV}5}, \Delta P_t^{\text{PV}4}] \cup [\Delta P_t^{\text{PV}4}, \Delta P_t^{\text{PV}5}]$ , there is a substantial amplitude; hence, non-spinning reserve units must be started, or some units must be shut down to achieve power balance within a specific period. Operators must start or stop the units in the appropriate time sequence to ensure that the reserve capacity remains within a reasonable range while maintaining the power balance. PV power fluctuation events in this range significantly impact the stability of the power system, leading to Level II warnings.
- 6)  $\Delta P_t^{\text{PV}} \in [-\Delta P_0^{\text{PV}}, \Delta P_t^{\text{PV}5}] \cup [\Delta P_t^{\text{PV}5}, P_{\text{max}}^{\text{PV}} - \Delta P_0^{\text{PV}}]$  indicates that during the specified period, all power adjustment measures mentioned above are insufficient to achieve a power balance. Consequently, PV curtailment or load shedding must be implemented. In the event of an upward fluctuation, resorting to PV curtailment results in a significant waste of energy resources, leading to an increase in the cost of power system operation. Conversely, in the case of downward fluctuations, load-shedding measures must be implemented, which may cause local power outages and severely affect the reliability of the power system. Therefore,

PV power fluctuation events within this range have a severe impact on the economy and reliability of the power system, warranting the highest level of warning, classified as Level I warnings.

### 3.2 | Probabilistic representation of multi-level warning levels for PV power fluctuation events

The PV power fluctuation amplitude is expressed in the form of an interval number, which allows the probability that the PV power fluctuation amplitude falls within different warning intervals to be calculated. The probabilities of the other warning levels for the DPPF can be expressed as

$$F_I = \int_{\min\{\Delta_{\underline{P}}^{\text{pv}5}, \Delta_{\underline{P}}^{\text{pv}}\}}^{\Delta_{\underline{P}}^{\text{pv}5}} f_{\Delta_{\text{P}^{\text{pv}}}}(P) dP + \int_{\Delta_{\underline{P}}^{\text{pv}5}}^{\max\{\Delta_{\underline{P}}^{\text{pv}5}, \Delta_{\underline{P}}^{\text{pv}}\}} f_{\Delta_{\text{P}^{\text{pv}}}}(P) dP; \quad (38)$$

$$F_{II} = \int_{\min\{\Delta_{\underline{P}}^{\text{pv}4}, \max\{\Delta_{\underline{P}}^{\text{pv}5}, \Delta_{\underline{P}}^{\text{pv}}\}\}}^{\Delta_{\underline{P}}^{\text{pv}4}} f_{\Delta_{\text{P}^{\text{pv}}}}(P) dP + \int_{\Delta_{\underline{P}}^{\text{pv}4}}^{\max\{\Delta_{\underline{P}}^{\text{pv}4}, \min\{\Delta_{\underline{P}}^{\text{pv}5}, \Delta_{\underline{P}}^{\text{pv}}\}\}} f_{\Delta_{\text{P}^{\text{pv}}}}(P) dP; \quad (39)$$

$$F_{III} = \int_{\min\{\Delta_{\underline{P}}^{\text{pv}3}, \max\{\Delta_{\underline{P}}^{\text{pv}4}, \Delta_{\underline{P}}^{\text{pv}}\}\}}^{\Delta_{\underline{P}}^{\text{pv}3}} f_{\Delta_{\text{P}^{\text{pv}}}}(P) dP + \int_{\Delta_{\underline{P}}^{\text{pv}3}}^{\max\{\Delta_{\underline{P}}^{\text{pv}3}, \min\{\Delta_{\underline{P}}^{\text{pv}4}, \Delta_{\underline{P}}^{\text{pv}}\}\}} f_{\Delta_{\text{P}^{\text{pv}}}}(P) dP; \quad (40)$$

$$F_{IV} = \int_{\min\{\Delta_{\underline{P}}^{\text{pv}2}, \max\{\Delta_{\underline{P}}^{\text{pv}3}, \Delta_{\underline{P}}^{\text{pv}}\}\}}^{\Delta_{\underline{P}}^{\text{pv}2}} f_{\Delta_{\text{P}^{\text{pv}}}}(P) dP + \int_{\Delta_{\underline{P}}^{\text{pv}2}}^{\max\{\Delta_{\underline{P}}^{\text{pv}2}, \min\{\Delta_{\underline{P}}^{\text{pv}3}, \Delta_{\underline{P}}^{\text{pv}}\}\}} f_{\Delta_{\text{P}^{\text{pv}}}}(P) dP; \quad (41)$$

$$F_V = \int_{\min\{\Delta_{\underline{P}}^{\text{pv}1}, \max\{\Delta_{\underline{P}}^{\text{pv}2}, \Delta_{\underline{P}}^{\text{pv}}\}\}}^{\Delta_{\underline{P}}^{\text{pv}1}} f_{\Delta_{\text{P}^{\text{pv}}}}(P) dP + \int_{\Delta_{\underline{P}}^{\text{pv}1}}^{\max\{\Delta_{\underline{P}}^{\text{pv}1}, \min\{\Delta_{\underline{P}}^{\text{pv}2}, \Delta_{\underline{P}}^{\text{pv}}\}\}} f_{\Delta_{\text{P}^{\text{pv}}}}(P) dP; \quad (42)$$

$$F_{\text{non}} = 1 - F_I - F_{II} - F_{III} - F_{IV} - F_V, \quad (43)$$

where  $f_{\Delta_{\text{P}^{\text{pv}}}}$  is the probability density distribution of the PV power fluctuation amplitude between the upper and lower limits of the prediction;  $F_I$ ,  $F_{II}$ ,  $F_{III}$ ,  $F_{IV}$ , and  $F_V$  represent the probabilities of the DPPF amplitudes falling within level I, II, III, IV, and V warning intervals, respectively, and  $F_{\text{non}}$  denotes the probability of no warning being required.

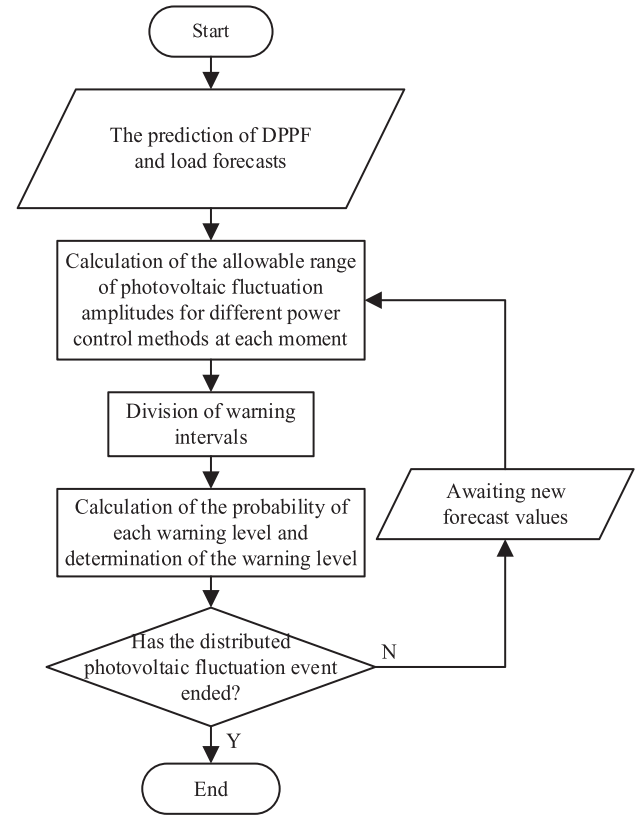


FIGURE 1 DPPF event multi-level interval rolling warning process diagram.

Suppose that the prediction error of PV power fluctuation amplitude follows a normal distribution [31–33], it can be expressed as

$$\Delta P_t^{\text{pv}} \sim N(\mu, \sigma^2), \quad (44)$$

where  $\mu$  and  $\sigma^2$  represent the expected value and variance of DPPF, respectively. Assuming that the confidence interval for the confidence level  $1 - \alpha$  is  $[\Delta_{\underline{P}}^{\text{pv}}, \Delta_{\underline{P}}^{\text{pv}}]$ , then the variance of the DPPF is  $\sigma^2 = (\Delta_{\underline{P}}^{\text{pv}} - \Delta_{\underline{P}}^{\text{pv}}) / (2Z_{\alpha/2})$ .

### 3.3 | Multi-level interval rolling warning for PV power fluctuation events

The rolling warning process is illustrated in Figure 1. The primary steps are as follows:

- 1) Obtain the forecast values of the DPPF and load forecasts. Calculate the allowable interval for the DPPF for different power control methods at each moment based on Equations (1)–(37) or the revised Equations (45) and (46).
- 2) Divide the allowable interval for the DPPF obtained in step 1 into five warning levels. Calculate the probability of each potential warning level according to Equations (38)–(43) and determine the warning level.

**TABLE 1** Parameters of the thermal units.

Unit number	Maximum allowable output (MW)	Minimum allowable output (MW)	Minimum startup time (h)	Minimum shutdown time (h)	Ramp rate ( $P_{\max}/h$ )
1	455	150	8	8	20%
2	455	150	8	8	20%
3	130	20	5	5	20%
4	130	20	5	5	20%
5	162	25	6	6	20%
6	80	20	3	3	20%
7	85	25	3	3	20%
8	55	10	1	1	20%
9	55	10	1	1	20%
10	55	10	1	1	20%

- 3) Determine whether the DPPF event has ended. If not, await new forecasted values and proceed to step 1 to recalibrate the warning results; if so, conclude the process.

Using the predicted PV power fluctuation forecast data and the operating status of the units in the previous period, the warning limits and results of each warning interval are updated. For example, if rewarning is performed at time  $t_1$ , the maximum and minimum adjustments  $\Delta P_{j,t_1}^{\max,1}$  and  $\Delta P_{j,t_1}^{\min,1}$  of the AGC unit  $j$  are modified from Equations (10) and (11) as follows:

$$\Delta P_{j,t_1}^{\max,1} = \min \left\{ P_j^{\max} - P_{j,0}, \Delta P_{j,(t_1-\Delta t)}^{\text{real,min},0} + R_j \Delta t \right\}; \quad (45)$$

$$\Delta P_{j,t_1}^{\min,1} = \max \left\{ P_j^{\min} - P_{j,0}, \Delta P_{j,(t_1-\Delta t)}^{\text{real,max},0} - R_j \Delta t \right\}, \quad (46)$$

where  $\Delta P_{j,(t_1-\Delta t)}^{\text{real,max},0}$  and  $\Delta P_{j,(t_1-\Delta t)}^{\text{real,min},0}$  are the maximum and minimum actual adjustments of the AGC unit  $j$  at time  $t_1 - \Delta t$ , respectively.

Similarly, equivalent modifications can be made to Equations (12)–(15) and (27)–(28). This approach enables rolling warnings and the correction of warning results.

## 4 | CASE STUDIES

In this study, a power system with ten conventional thermal units [34, 35] was used to validate the effectiveness of the proposed method. The detailed parameters of these units are listed in Table 1. The lower-level distribution network of the system has a total capacity of 600 MW for the DPV system. All conventional units participate in the primary frequency regulation, where units 1 to 4 are AGC units. The governor droop of each unit is 5%, the load-damping coefficient is 1% [36], and the allowable range of the power system frequency deviation is  $\pm 0.1$  Hz. Assume that the load and the PV power fluctuation forecasting errors are 2% and 15%, respectively. Calculations for the case study were performed using MATLAB R2022a.

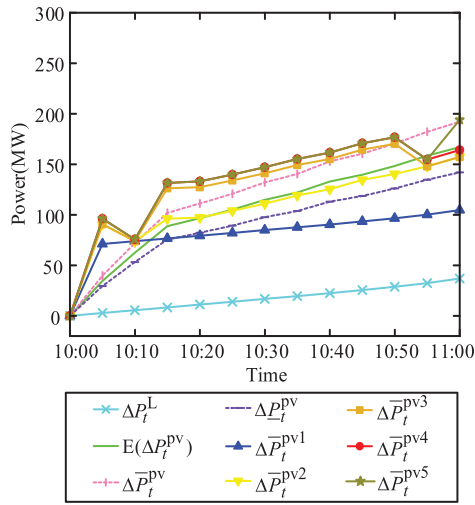
### 4.1 | Warning results of the PV power fluctuation events

Three cases were designed to test the effectiveness of the proposed approach. In Case 1, we assumed that a DPPF event with an upward amplitude of 30% of the total output power of the conventional units would occur from 10:00 am. Such extreme events are primarily caused by weather conditions like intense sunlight. The DPPF event warning was updated every 10 min based on new PV forecasting data. The predicted load followed a bimodal curve with peaks at 12:00 and 18:00 h, which is the load of a typical urban area. Four warnings were issued in this case, at 10:00, 10:10, 10:20, and 10:30 am, and the results are shown in Figures 2–5. The computation time of the proposed method was 0.42865 s.

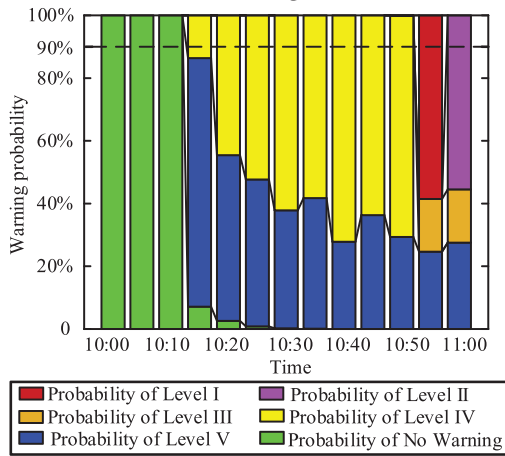
As shown in Figure 2a, from 10:00–10:10 am, a power balance was achieved through primary frequency regulation. From 10:15 am onwards, the effects of the primary and secondary frequency regulations were insufficient to meet the power balance requirements. Power balance can be achieved by charging and discharging the energy storage system. However, after 10:50 am, owing to the capacity limitations of the energy storage system, it becomes fully charged and is unable to maintain the power balance. At 10:55 am, even an increased dispatch of spinning reserve units could not ensure power balance. Because non-spinning reserves cannot be activated at this time, power balance can only be achieved by curtailing PV generation. By 11:00 am, with the activation of non-spinning reserves, the system can achieve a power balance through these measures.

The PV forecast fluctuation was assumed to follow a normal distribution with a confidence level of 90%. Using interval ranking methods to determine the probability density of the DPPF within each warning interval, the probabilities of PV power fluctuations falling within each warning level were obtained, as shown in Figures 2b, 3b, 4b, and 5b.

Assuming a risk-warning threshold of 10%, the warning process can be divided into four stages, as shown in Figure 2b. In Stage 1, from 10:00 to 10:10 am, no warnings were generated.



(a) PV power fluctuation amplitude and boundary curves of each warning level



(b) Probability of each warning level

FIGURE 2 Warning results at 10:00 am for Case 1.

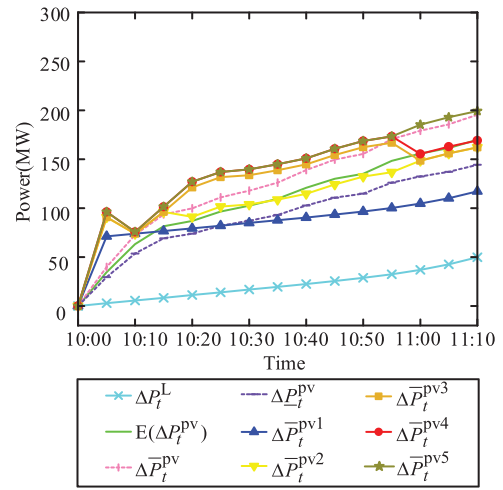
In Stage 2, from 10:10 to 10:50 am, the probability of generating a Level IV warning or above exceeded 10%, placing the system in a Level IV warning state. From 10:50 to 10:55 am, the system entered Stage 3, and from 10:55 to 11:00 am, it transitioned to Stage 4, corresponding to Level I and II warning states.

## 4.2 | Validity analysis

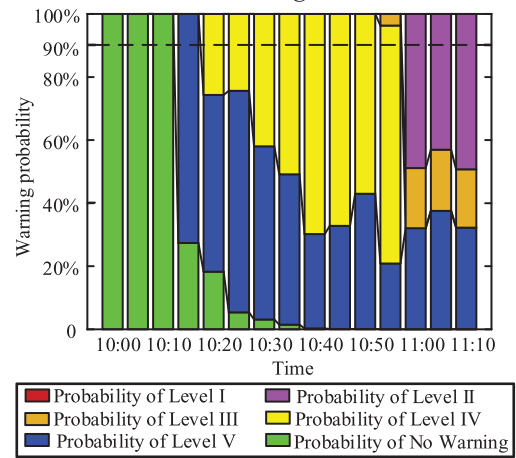
The system parameters, DPPF events, and load conditions were varied, and their impact on the warning results was analysed to verify the effectiveness of the proposed warning method.

### 4.2.1 | Impact of different system parameters

In Case 2, unit 5 is changed to an AGC unit, and the minimum downtime of units 9 and 10 is reduced to 0.5 h to allow for early participation in response to PV power fluctuations. The PV power fluctuations and load forecast data remained the same



(a) PV power fluctuation amplitude and boundary curves of each warning level



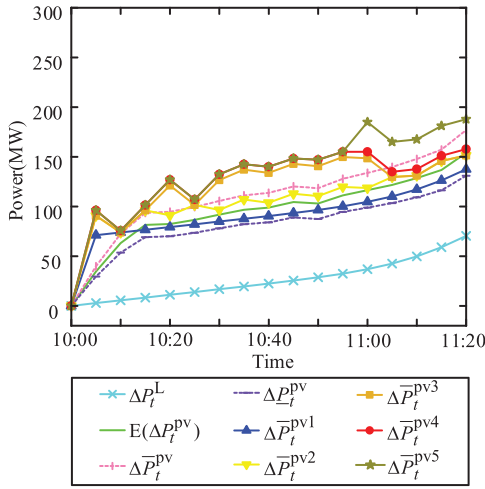
(b) Probability of each warning level

FIGURE 3 Warning results at 10:10 am for Case 1.

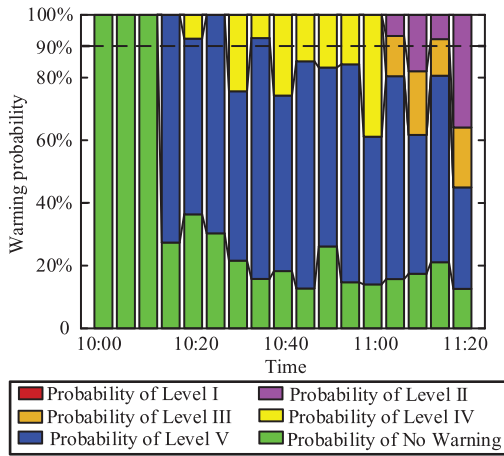
as in Case 1. The warning results at 10:00 am are shown in Figure 6.

Comparing Figures 6a and 2a, it can be observed that the upper limit of the fluctuation allowed by the secondary frequency regulation slightly increased. This is because the addition of AGC units in Case 2 increases the regulating rate and adjustable capacity of the secondary frequency regulation. The upper limit curve of the non-spinning reserve zone experiences a stepwise upward shift at 10:30 am owing to the earlier shutdown of units 9 and 10.

Comparing Figures 6b with 2b, the overall probability of Level III warnings decreases significantly, primarily because of the upward shift in  $\Delta P_t^{pv2}$ . Additionally, the Level I warning predicted to occur between 10:50 am and 10:55 am in Case 1 was changed to a Level II warning because of the earlier shutdown of Units 9 and 10. Thus, it can be concluded that for systems with high penetration of distributed PVs, increasing the number of AGC units or reducing the start/stop time of units can contribute to achieving power balance in the power system, thereby improving the stability and flexibility of the power system.

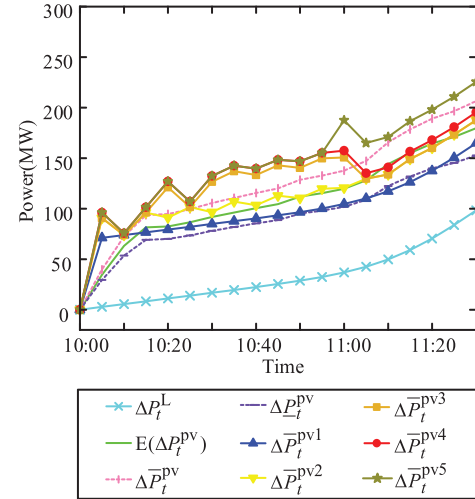


(a) PV power fluctuation amplitude and boundary curves of each warning level

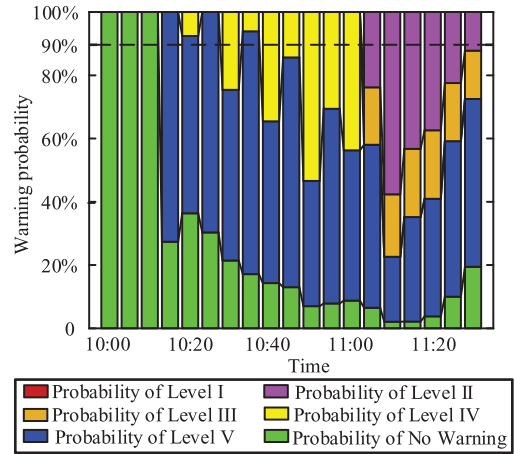


(b) Probability of each warning level

FIGURE 4 Warning results at 10:20 am for Case 1.



(a) PV power fluctuation amplitude and boundary curves of each warning level



(b) Probability of each warning level

FIGURE 5 Warning results at 10:30 for Case 1.

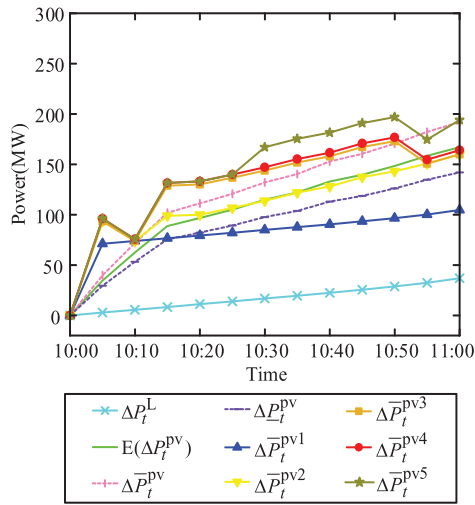
### 4.2.2 | Impact of different PV power fluctuation event occurrence times

In Case 3, the load curve changed to a typical bimodal curve in the industrial area, with load peaks at 6:00 and 18:00. The load variation changed from increasing to decreasing, whereas the other data remained the same as in Case 1. The warning results at 10:00 a.m. are shown in Figure 7.

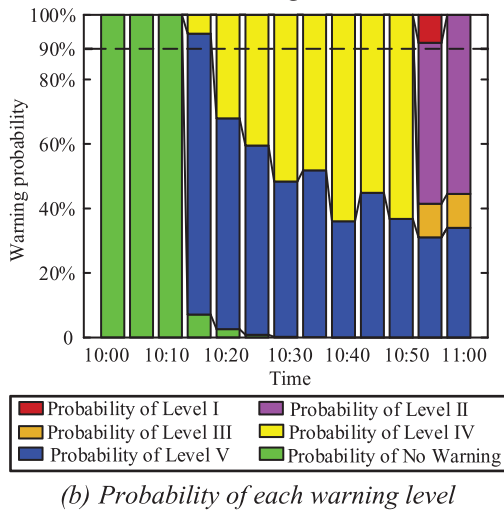
In Case 1, the load and PV power fluctuations were in the same direction, partially offsetting each other, and resulting in a slower net load variation, leading to a relatively lower severity of warnings. In Case 3, however, the load demand gradually decreased while the PV output increased, resulting in an increased net load variation and increased difficulty in achieving a power balance. A comparison of Figures 7b and 2b shows that the probability of higher-level warnings significantly increases. For example, between 10:45 and 10:50, the likelihood of a level I warning in Case 1 was nonexistent. However, Case 3 showed approximately a 50% chance of a Level I warning occurring. This was because of the charging and discharging being shifted

5 min earlier, resulting in the battery reaching full charging sooner. This indicates that the impact of PV power fluctuation events on power system stability varies depending on the scenario. Therefore, it is necessary to analyse the characteristics of PV power fluctuation events and load demand variations to accurately assess the severity of DPPF events and assign appropriate warning levels.

In conclusion, the warning method proposed in this study allows the analysis of the impact of different system parameters and DPPF events. By analysing the allowed upper/lower limits of PV power fluctuation and calculating the probability of PV power fluctuations falling into each warning level, the proposed method enables operators to understand the severity of DPPF events and take appropriate measures in advance, avoiding misjudgment caused by considering only extreme scenarios and minimizing the adverse effects of extreme events on power system stability. However, this method has certain limitations. It does not consider the network topology of the actual system and ignores network security constraints during the calculation process. Consequently, the proposed method can only provide



(a) PV power fluctuation amplitude and boundary curves of each warning level



(b) Probability of each warning level

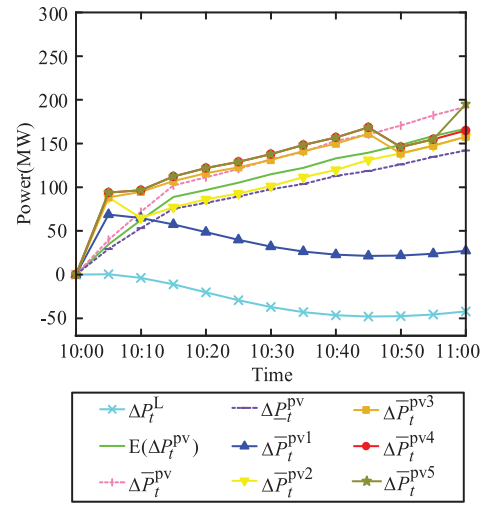
FIGURE 6 Warning results at 10:00 am for Case 2.

warnings for risks, such as potential PV curtailment and load shedding, caused by the DPPF, without reflecting the risk of line overload.

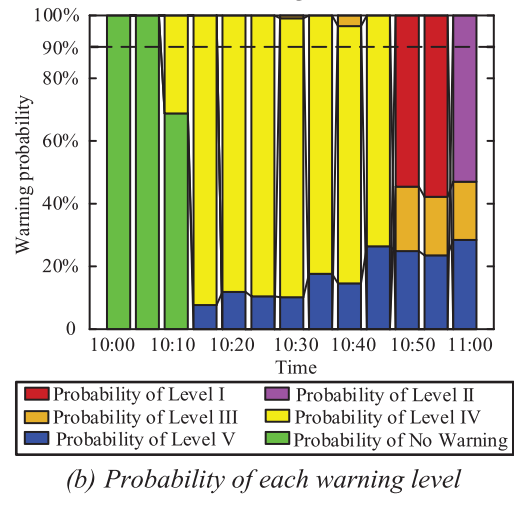
## 5 | CONCLUSION

In response to the power balance challenges caused by DPPF, this study proposes a multi-level rolling warning method for PV power fluctuation events based on interval analysis.

1. The allowable ranges of PV power fluctuations for power control measures, including primary frequency modulation, secondary frequency modulation, energy storage system charging and discharging, spinning reserve, non-spinning reserve, and PV curtailment or load shedding, were determined, thereby obtaining the warning limits corresponding to each warning level.
2. The probability of each warning interval can be obtained using the proposed method, which allows operators to take



(a) PV power fluctuation amplitude and boundary curves of each warning level



(b) Probability of each warning level

FIGURE 7 Warning results at 10:10 for Case 3.

corresponding measures according to the warning status to mitigate the impact of the DPPF. Additionally, rolling warnings of DPPF events based on the latest PV forecast data can effectively improve the reliability and accuracy of the warning results.

3. For different system operation statuses and different PV power fluctuation events, the proposed method can perform multi-level rolling warnings, which verifies the effectiveness and applicability of the technique.

The proposed method has practical significance in enhancing the stability of power systems with a high proportion of distributed PV generation.

## CONFLICT OF INTEREST STATEMENT

The authors declare no conflicts of interest.

## DATA AVAILABILITY STATEMENT

Research data are not shared.

## ORCID

Yumin Zhang  <https://orcid.org/0000-0002-9159-0290>

Pingfeng Ye  <https://orcid.org/0009-0002-2247-9246>

Jiajia Yang  <https://orcid.org/0000-0002-3829-4302>

## REFERENCES

- Yu, S., Han, R., Zhang, J.: Reassessment of the potential for centralized and distributed photovoltaic power generation in China: on a prefecture-level city scale. *Energy* 262, 125436 (2023)
- Ji, X., Zhang, X., Ye, P., et al.: Dynamic reconfiguration of three-phase imbalanced distribution networks considering soft open points. *Energy Convers. Econ.* 4(5), 364–377 (2023)
- Ge, L., Du, T., Li, C., et al.: Virtual collection for distributed photovoltaic data: challenges, methodologies, and applications. *Energies* 15(23), 8783 (2022)
- Jiang, S., Wan, C., Chen, C., et al.: Distributed photovoltaic generation in the electricity market: status, mode and strategy. *CSEE J. Power Energy Syst.* 4(3), 263–272 (2018)
- Huang, N., Zhao, X., Guo, Y., et al.: Distribution network expansion planning considering a distributed hydrogen-thermal storage system based on photovoltaic development of the whole county of China. *Energy* 278, 127761 (2023)
- Li, J., Wang, J., Lu, L., et al.: Research on distributed photovoltaic day-ahead scheduling and consumption strategy. In: 2022 4th International Conference on Power and Energy Technology (ICPET), pp. 753–758. IEEE, Piscataway, NJ (2022)
- Wang, K., Wang, C., Yao, W., et al.: Embedding P2P transaction into demand response exchange: a cooperative demand response management framework for IES. *Appl. Energy* 367, 123319 (2024)
- Impram, S., Nese, S.V., Oral, B.: Challenges of renewable energy penetration on power system flexibility: a survey. *Energy Strat. Rev.* 31, 100539 (2020)
- Zhang, Y., Li, J., Ji, X., et al.: Optimal dispatching of electric-heat-hydrogen integrated energy system based on Stackelberg game. *Energy Convers. Econ.* 4(4), 267–275 (2023)
- Zhao, Q., Yang, A., Ma, H., et al.: Hybrid scheduling strategy based on new energy consumption and optimal operation cost. In: 2022 IEEE 5th International Electrical and Energy Conference (CIEEC), pp. 906–911. IEEE, Piscataway, NJ (2022)
- Yan, J., Li, C., Liu, Y.: Insecurity early warning for large scale hybrid AC/DC grids based on decision tree and semi-supervised deep learning. *IEEE Trans. Power Syst.* 36(6), 5020–5031 (2021)
- Liu, X., Liu, J., Zhao, Y., et al.: A Bayesian deep learning-based probabilistic risk assessment and early-warning model for power systems considering meteorological conditions. *IEEE Trans. Ind. Inf.* 20(2), 1516–1527 (2023)
- Bai, F., Liu, Y., Liu, Y., et al.: A measurement-based approach for power system instability early warning. *Prot. Control Mod. Power Syst.* 1(1), 1–9 (2016)
- Manickavasagam, K., Prasad, B.K.S., Ramasangu, H.: Assessment of power system security using security information index. *IET Gener. Transm. Distrib.* 13(14), 3040–3047 (2019)
- Ryo, E.: A study of system frequency control of island power network using disturbance observer with adaptive behavior controller. In: Proceedings of the International Conference on Electrical Engineering, pp. 43–48. IEEE, Piscataway, NJ (2009)
- Yan, X., Huan, X.: An improved power planning model based on electric power and clean energy substitution. In: 2017 2nd International Conference on Power and Renewable Energy (ICPRE), pp. 671–675. IEEE, Piscataway, NJ (2017)
- Li, J., Li, J., Zeng, X., et al.: Power balance warning method of regional power grid considering photovoltaic capacity ratio. In: 2023 IEEE 7th Information Technology and Mechatronics Engineering Conference (ITOC), vol. 7, pp. 133–137. IEEE, Piscataway, NJ (2023)
- Zheng, W., Wu, W., Zhang, B., et al.: A fully distributed reactive power optimization and control method for active distribution networks. *IEEE Trans. Smart Grid* 7(2), 1021–1033 (2016)
- Shi, J., Chen, Y., Cheng, X., et al.: Four-stage space-time hybrid model for distributed photovoltaic power forecasting. *IEEE Trans. Ind. Appl.* 59(1), 1129–1138 (2022)
- Das, U.K., Tey, K.S., Seyedmahmoudian, M., et al.: Forecasting of photovoltaic power generation and model optimization: a review. *Renewable Sustainable Energy Rev.* 81, 912–928 (2018)
- Si, Z., Yang, M., Yu, Y., et al.: Photovoltaic power forecast based on satellite images considering effects of solar position. *Appl. Energy* 302, 117514 (2021)
- Ahmed, R., Sreeram, V., Mishra, Y., et al.: A review and evaluation of the state-of-the-art in PV solar power forecasting: techniques and optimization. *Renewable Sustainable Energy Rev.* 124, 109792 (2020)
- Li, Y., Yang, Z., Li, G., et al.: Optimal scheduling of an isolated micro-grid with battery storage considering load and renewable generation uncertainties. *IEEE Trans. Ind. Electron.* 66(2), 1565–1575 (2018)
- Su, Y., Liu, F., Wang, Z., et al.: Multi-stage robust dispatch considering demand response under decision-dependent uncertainty. *IEEE Trans. Smart Grid* 14(4), 2786–2797 (2022)
- Wang, Y., Shi, J., Ma, Y., et al.: Ultra-short-term interval prediction model for photovoltaic power based on bayesian optimization. In: 2022 IEEE/IAS Industrial and Commercial Power System Asia (I&CPS Asia), pp. 1138–1144. IEEE, Piscataway, NJ (2022)
- Zhang, J., Liu, Z., Chen, T.: Interval prediction of ultra-short-term photovoltaic power based on a hybrid model. *Electr. Power Syst. Res.* 216, 109035 (2023)
- Moon, J., Park, J., Hwang, E., et al.: Forecasting power consumption for higher educational institutions based on machine learning. *J. Supercomput.* 74, 3778–3800 (2018)
- Jia, Y., Kwong, S., Wu, W., et al.: Sparse Bayesian learning-based kernel poisson regression. *IEEE Trans. Cybern.* 49(1), 56–68 (2017)
- Mitali, J., Dhinakaran, S., Mohamad, A.A.: Energy storage systems: a review. *Energy Storage Saving* 1(3), 166–216 (2022)
- Elalfy, D.A., Gouda, E., Kotb, M.F., et al.: Comprehensive review of energy storage systems technologies, objectives, challenges, and future trends. *Energy Strat. Rev.* 54, 101482 (2024)
- Ziadi, Z., Oshiro, M., Senjyu, T., et al.: Optimal voltage control using inverters interfaced with PV systems considering forecast error in a distribution system. *IEEE Trans. Sustainable Energy* 5(2), 682–690 (2014)
- Zhao, W., Zhang, N., Kang, C., et al.: A method of probabilistic distribution estimation of conditional forecast error for photovoltaic power generation. *Autom. Electr. Power Syst.* 39(16), 8–15 (2015)
- Liu, Y., Hu, C., Miao, M., et al.: Different terms fluctuations of solar power system. In: 2016 4th International Conference on Machinery, Materials and Information Technology Applications, pp. 1300–1306. Atlantis Press, Dordrecht (2017)
- Kazarlis, S.A., Bakirtzis, A.G., Petridis, V.: A genetic algorithm solution to the unit commitment problem. *IEEE Trans. Power Syst.* 11(1), 83–92 (1996)
- Kumar, N., Panigrahi, B.K., Singh, B.: A solution to the ramp rate and prohibited operating zone constrained unit commitment by GHS-JGT evolutionary algorithm. *Int. J. Electr. Power Energy Syst.* 81, 193–203 (2016)
- Glover, J.D., Overbye, T.J., Sarma, M.S.: *Power System Analysis & Design*. Cengage Learning, Boston, MA (2017)

**How to cite this article:** Zhang, Y., Qi, Y., Ye, P., Li, Z., Yang, J., Ji, X.: Multi-level interval rolling warning method for distributed photovoltaic fluctuation events. *Energy Convers. Econ.* 5, 370–381 (2024). <https://doi.org/10.1049/enc2.12133>